

Large Scale Numerical Simulations of Galaxy Formation

Ryoji Matsumoto^{1*}, Masao Mori² and Masayuki Umemura³

¹ Department of Physics, Faculty of Science, Chiba University, 1-33 Yayoi-Cho, Inage-ku Chiba 263-8522, Japan

² Institute of Natural Sciences, Senshu University, Kawasaki, Kanagawa 214-8580, Japan

³ Center for Computational Science, University of Tsukuba, Tsukuba, Ibaraki 305-8577, Japan

(Received December 28, 2004; Revised manuscript accepted February 27, 2004)

Abstract We present the results of high-resolution (1024^3 grid) three-dimensional simulations of the formation of a galaxy based on the bottom-up scenario, in which a galaxy is built up by an assemblage of a numerous sub-galactic systems. Each sub-galactic system is composed of dark matter and the primordial gas confined by the gravitational potential of the dark matter. The motion of the dark matter clumps is traced by numerically solving the N-body problem. The dynamics of the gas component is simulated by applying a parallelized compressible fluid dynamic code AFD2 based on the finite volume (AUSMDV+MUSCL) method. The multiple supernovae in the primordial galaxy produce expanding hot bubbles surrounded by a cool dense shell. The gas in the vicinity of supernovae is highly polluted with synthesized heavy elements. By using a spectral synthesis code for an astrophysical plasma, we visualized the Ly α emission from the forming galaxy. We find that the luminosity and the distribution of the Ly α emission from the simulated galaxy reproduce those of the Ly α emitters recently observed by Subaru telescope.

Keywords: Astrophysics, hydrodynamics, galaxy formation, hierarchical structure

1. Introduction

The universe has hierarchical structure consisting of stars, galaxies, cluster of galaxies, and the large-scale structure. More than 80% of the gravitating mass in the universe is invisible matter called the dark matter. The left panel of figure 1 shows a result of the N-body simulation using 512^3 particles carried out by H. Yahagi of the evolution of the dark matter distribution in the expanding universe [1]. The gravitationally interacting dark matter forms filamentary distributions known as the large-scale structure of the universe. The middle panel of figure 1 enlarges a local part of the left panel where sub-clumps of the dark matter form a cluster of dark matter condensations. The gas trapped in the gravitational potential of dark matter clumps forms galaxies consisting of stars and the interstellar gas (right panel of figure 1).

Figure 2 shows interactions linking the hierarchical structures of the universe. Through gravitational, hydrodynamic, hydromagnetic, and electromagnetic interactions, a local sub-system can affect the dynamics and evolution of the whole system. Dark matters interact with the interstellar/intercluster matter and stars through gravitational attraction. Hydrodynamical instabilities such as

the gravitational instability enables a local part of the interstellar matter to collapse and form stars. When a star explodes as a supernova, chemically enriched gas is ejected into the interstellar/intercluster space. Thus, the interstellar gas is recycled by supernova explosions. Shock waves created by the supernova explosion affect the gas dynamics of the whole galaxy. Stars also affect the evolution of the interstellar matter by ionizing them through radiation. Another mechanism linking the hierarchical structure is magnetic interactions.

Due to the limitation of computational capabilities, each level of the hierarchical structure of the universe had been simulated separately. The Earth Simulator gives us a unique opportunity to carry out global simulations including multiple levels of the hierarchy in the computational domain.

In this paper, we present the results of large-scale numerical simulations of a galaxy formation based on a bottom-up scenario, in which a galaxy is built up by an assemblage of numerous sub-galactic systems. We include the effects of star formation and supernova explosions in each sub-galactic system.

* **Corresponding author:** Dr. Ryoji Matsumoto, Department of Physics, Faculty of Science, Chiba University, 1-33 Yayoi-Cho, Inage-ku Chiba 263-8522, Japan, E-mail: matumoto@astro.s.chiba-u.ac.jp

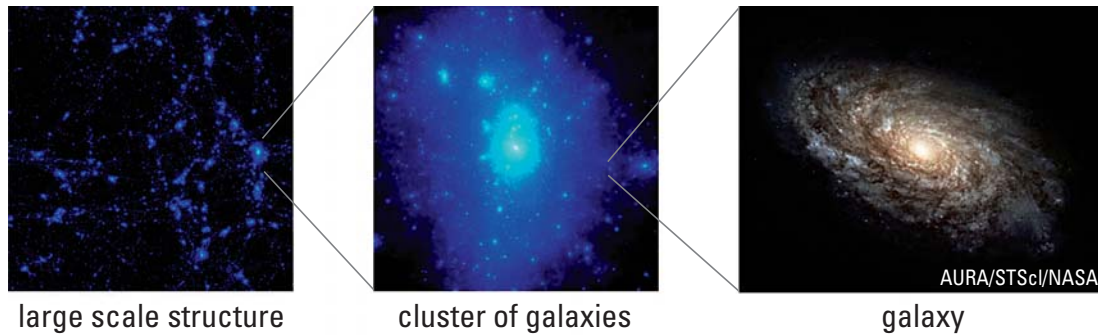


Fig. 1 Hierarchical structure of the universe. The left and middle panels show the results of the N-body simulation carried out by H. Yahagi of the motion of dark matters in an expanding universe[1]. The middle panel enlarges a local part of the dark matter condensations. The right panel shows the Hubble Space Telescope image of a spiral galaxy NGC4414 (credit: AURA/STScI/NASA).

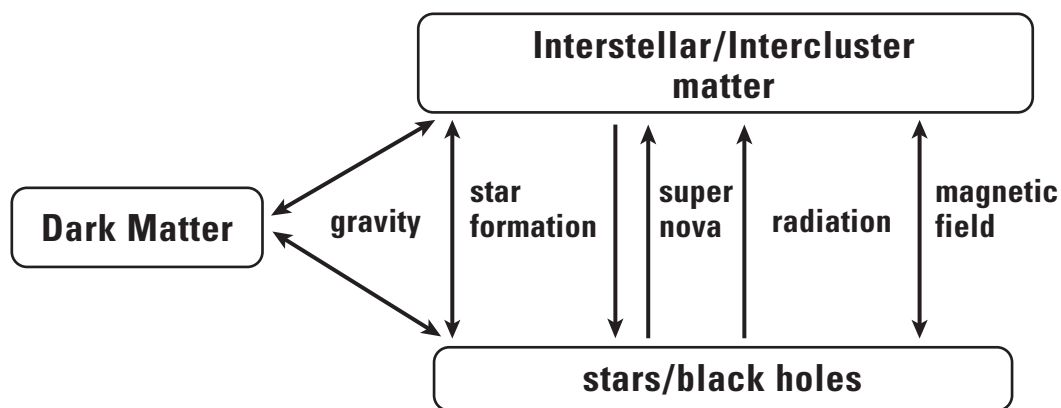


Fig. 2 Physical processes linking the hierarchical structures of the universe.

2. Hydrodynamic Simulations of Galaxy Formation

2.1 Bottom-up Scenario of Galaxy Formation

Our understanding of galaxy formation has greatly deepened in last decade due to multi-wavelength observations of distant star-forming galaxies. Optical observations have revealed the presence of a number of star-forming galaxies, so-called Lyman break galaxies. Lyman break galaxies are usually characterized by compact cores (some with multiple components) of 5-8 kpc ($1\text{pc} = 3.26$ light years) and often surrounded by more diffuse, asymmetric halos. A good fraction of these galaxies exhibit Ly α emission lines of the hydrogen atom strong enough to be detected by narrow band observations. Imaging observations using the Ly α emission lines revealed the existence of very luminous and extended Ly α nebulae, so-called Ly α blobs, which have the Ly α luminosity of more than 10^{43} ergs s^{-1} and the physical extent of about 100 kpc [2][3][4]. If these Ly α emitters are quite young galaxies, they could hold direct information on the early chemical enrichment of galaxies, contrary to present-day galaxies which have undergone recy-

cling of the interstellar medium, thus erasing most of the early chemical history.

In currently popular hierarchical clustering scenarios for the formation of cosmic structures, the assembly of galaxies is a bottom-up process in which large systems result from the merging of smaller subunits. Figure 3 schematically shows this scenario. In these theories dark matter clumps with masses $M=10^8 M_{\odot}$ (M_{\odot} is a solar mass) collapse at redshift $z=10$ (about 12Gyrs ago). The gas infalling along with the dark matter clumps is shock-heated, condenses rapidly due to atomic line cooling, and becomes self-gravitating. Massive stars then form, synthesize heavy-elements, and explode as supernovae after a few 10^7 yr, enriching the surrounding medium.

The deep optical spectroscopy of Ly α blobs suggests that the kinematical properties of Ly α emitters favor supernova driven winds [3]. Interestingly, Matsuda et al. [4] have revealed bubbly features in Ly α blobs, where the bubble size is typically 15 kpc. These bubbly structures strongly suggest that supernova events could be closely related to Ly α blobs. The complexes of various superbubbles, which can be driven by multiple supernovae, are

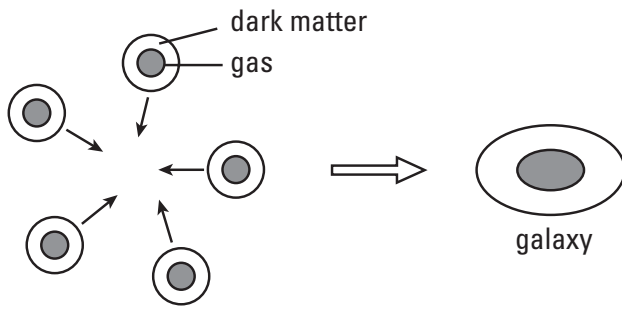


Fig. 3 A bottom-up scenario of galaxy formation

an attractive explanation for Ly α blobs. However, it has not been shown whether multiple supernova explosions can actually produce the observed Ly α emission. We attempt to build up a multiple supernova explosion model for Ly α blobs. For this purpose, we perform an ultra-high resolution (1024^3 grids) simulation of galaxy formation including the supernova explosions in inhomogeneous and multiphase interstellar matter. This is the first result of simulation of galaxy formation with sufficient spatial resolution to resolve individual supernovae remnants (~ 100 pc).

2.2 Numerical Model

We define a fiducial model for Ly α blobs, in which the total mass of gaseous matter is initially assumed to be $M_b = 1.3 \times 10^{10} M_\odot$ and the total mass including dark matter is $M_t = 10^{11} M_\odot$. We assume a cosmology with matter fraction $\Omega_M = 0.3$, fraction of dark energy $\Omega_\Lambda = 0.7$, baryon fraction $\Omega_b = 0.04$, and a Hubble constant of $h = 0.7$. According to the general picture of bottom-up scenarios for galaxy formation, we model a protogalaxy as an assemblage of numerous sub-galactic condensations building up the total mass of a galaxy. The galaxy as a whole is modeled as a system in a radius of 56 kpc. Sub-galactic condensations encompassing a mass of $2.0 \times 10^9 M_\odot$ in radius $R_s = 8.6$ kpc are then distributed randomly.

Our simulation uses a hybrid N -body/hydrodynamic code applicable to a complex system consisting of dark matters, stars and gas. The dark matter should be treated differently from gas because they are collisionless. Stars are also treated as collisionless particles because the collision frequency of stars in a galaxy is very small. Thus, even when two sub-galactic condensations collide, individual dark matters and stars do not collide. On the other hand, interstellar/intercluster gases are described by macroscopic quantities such as density, pressure, and velocity at each point. For simplicity, instead of solving the dynamics of individual dark matter particle, we represent the gravity of each sub-galactic clump by that of a macro-particle and computed the time evolution of the

macro-particles by solving the gravitational N -body problem. The basic equations for gas are those of compressible hydrodynamics consisting of conservation equations for density, momentum, and energy. These equations are solved by finite difference method. The gravity at each grid point is computed by summing the gravity of the macro-particles.

The gas is allowed to form stars and is subject to physical processes such as the radiative cooling and the energy feedback from supernovae and massive stars. Chemical and photometric evolution of the system can also be simulated by this code. The gas dynamics is pursued by a three-dimensional hydrodynamic scheme with 1024^3 Cartesian grids. The simulation box has a (physical) size of 120 kpc and the spatial resolution is 117 pc. The set of basic equations are numerically solved by a parallel version of the Astrophysical Fluid Dynamics (AFD2) code [5]. AFD2 is a compressible fluid dynamic code based on the finite volume (AUSMDV+MUSCL) method. Here, we employ the AUSM-DV scheme [6], which is a TVD scheme that can resolve the shock accurately. We adopted MPI and domain decomposition to parallelize the code. The parallelization ratio of AFD2 is more than 99.9%. The parallelization efficiency of AFD2 for 1024^3 grid simulations is 55.6% on 128 nodes of the Earth Simulator.

We use a tracer field advected with the same algorithm as the density in order to follow the metallicity of the gas. Also, the gas is assumed to be optically thin and in collisional ionization equilibrium. Radiative cooling losses are calculated self-consistently using the metallicity-dependent curves by Sutherland and Dopita [7].

Stars are assumed to form in rapidly cooling and Jeans unstable regions at a rate which is inversely proportional to the local free-fall time. When a star particle is formed, we identify this with approximately 10^4 single stars and distribute the associated mass of the star particle over the single stars according to Salpeter's initial mass function. The lower and upper mass limits are taken as $0.1 M_\odot$ and $50 M_\odot$, respectively. When a star particle is formed and identified with a stellar assemblage as described above, stars more massive than $8 M_\odot$ start to explode as Type II supernovae (SNe II) with the explosion energy of 10^{51} ergs and their outer layers are blown out with synthesized heavy elements leaving the remnant of $1.4 M_\odot$. A mass of $2.4 M_\odot$ of oxygen and of $9.1 \times 10^{-2} M_\odot$ of iron are ejected from a Type II SN explosion [8]. The ejected energy and well-mixed heavy elements by the supernova are supplied to 8 local cells surrounding the supernova region.

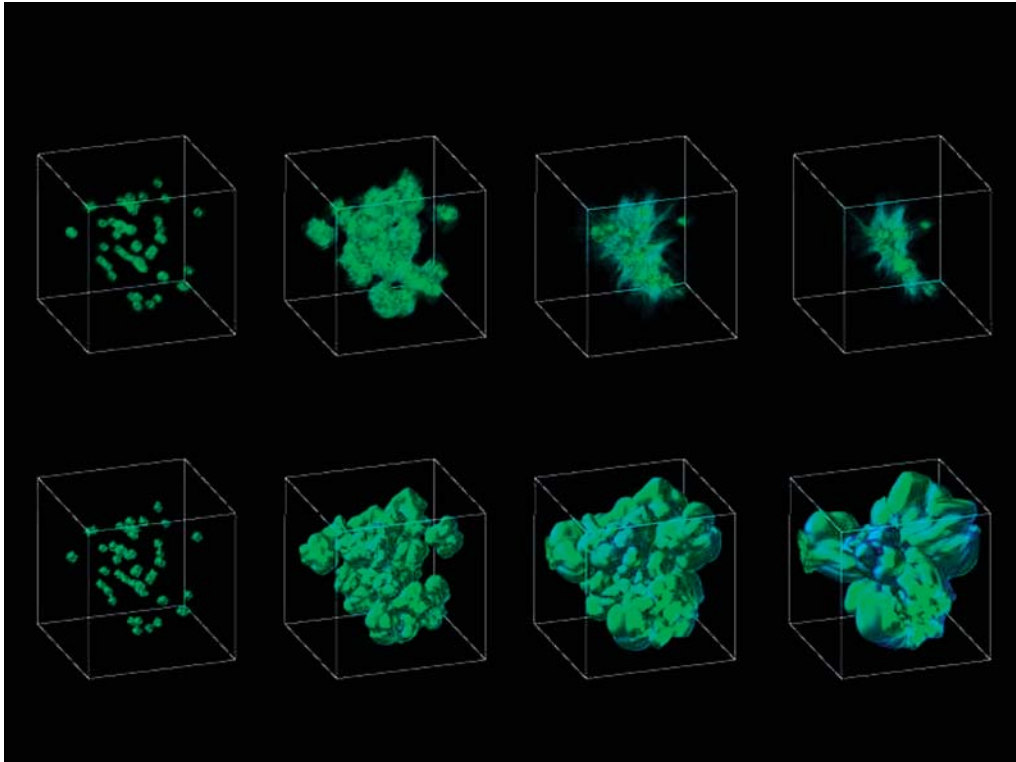


Fig. 4 Results of numerical simulation of galaxy formation. The panels show the snapshots for the distribution of density (upper panels) and metallicity (lower panels) at $t=0.01, 0.4, 0.8$ and 1.2 Gyr from left to right.

2.3 Numerical Results

Figure 4 shows the snapshots for the distribution of density (upper panels) and metallicity (lower panels) as a function of elapsed time. The efficient radiative cooling mainly through collisional excitation of H and He^+ , induces a dynamical contraction of gas by the gravity of dark matter. The density in the sub-galactic system increases by the accretion of the surrounding gas, and eventually the intensive star formation is triggered. After 10^8 yr from the beginning of the simulation, burst of star formation occurs and the most massive stars explode as supernovae and produce expanding hot bubbles surrounded by a cooling dense shell. Figure 5 shows the star formation history of the simulated galaxy. The peak star formation rate is about $40 M_{\odot} \text{ yr}^{-1}$ around 200 Myr and the burst of star formation continues to 300 Myr. Then the star formation rate gradually decreases down to a few $10 M_{\odot} \text{ yr}^{-1}$ after 500 Myr.

Snapshots of the gas density, the gas metallicity $[\text{O}/\text{H}]$ (the logarithm of the ratio of oxygen to hydrogen), and the gas temperature distributions in a slice along the X-Y plane are shown in Figure 6. The four panels in each low depict the time evolution from about 100 Myr to up to 1 Gyr. The density range is $-6 < \log(n/\text{cm}^{-3}) < 1$, the metallicity range is $-6 < [\text{O}/\text{H}] < 0$, and the temperature range is $4 < \log(T/\text{K}) < 7$. The gas temperature increas-

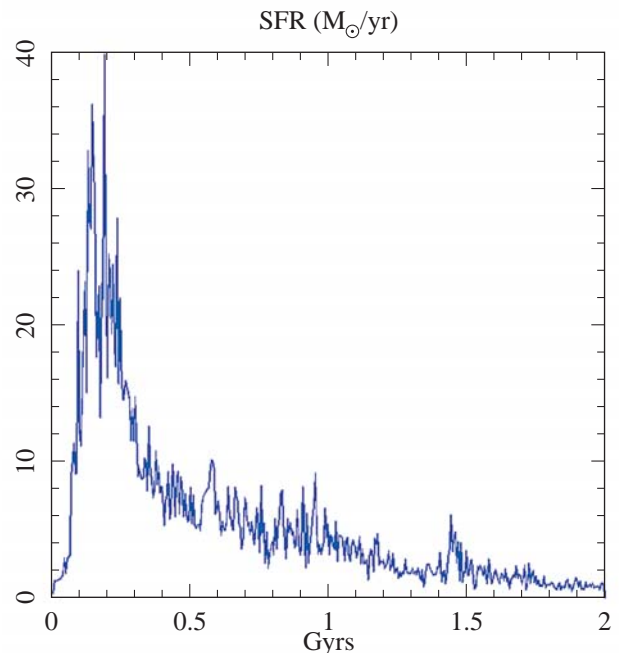


Fig. 5 Star formation history of the simulated galaxy.

es up to about 10^8 K locally, and expanding hot bubbles of kpc size are produced; they are enclosed by cooled, dense shells.

Subsequent supernova explosions further accelerate the expansion of hot bubbles and the ambient gas is continu-

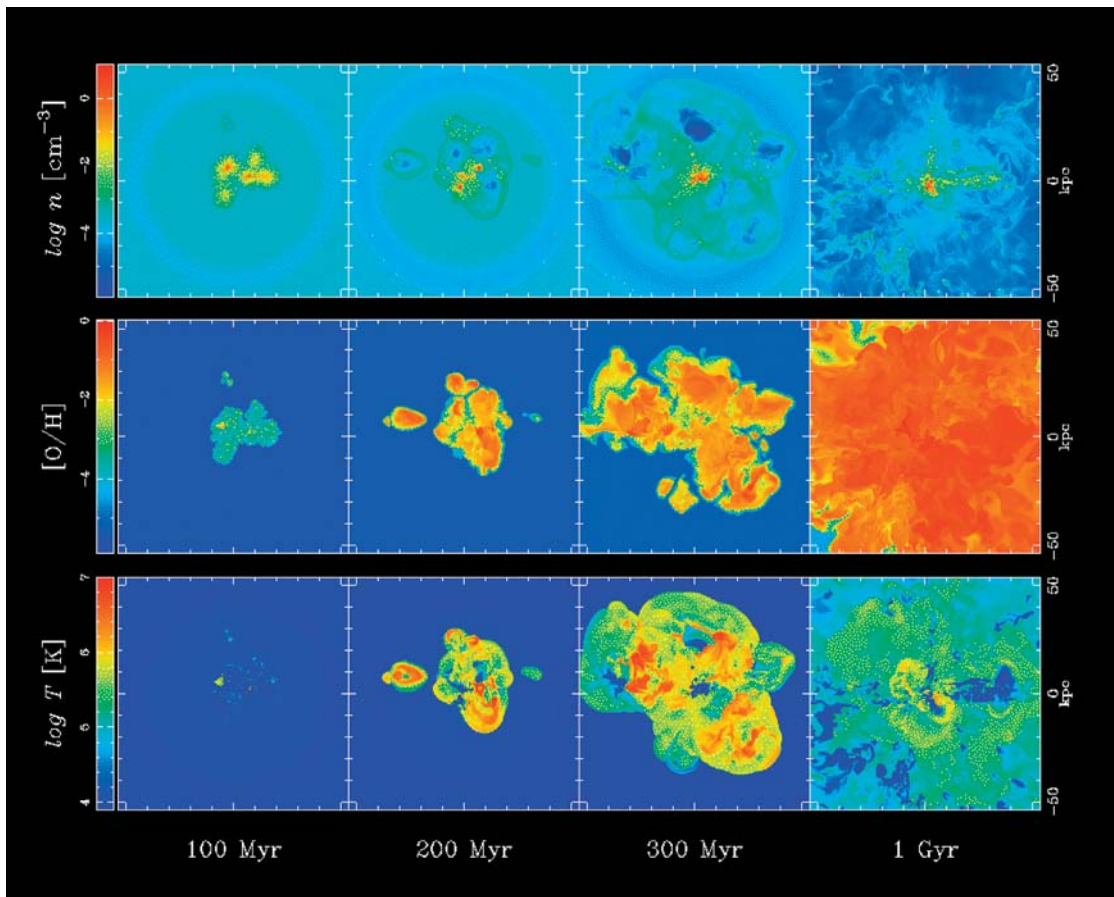


Fig. 6 Snapshots of the gas density, the gas metallicity [O/H], and the gas temperature distributions in a slice along the X-Y plane.

ously swept up by the shells; the gas density increases further owing to the enhanced cooling rate in the dense shells. Since in the outer regions the density of the interstellar matter is low, the bubble expansion is faster and supernova-driven shock waves quickly collide with each other to generate super-bubbles of 10 kpc size and the surrounding high-density, cooled shells eventually form. The different initial topology of the multiphase interstellar matter leaves an imprint also in the later evolutionary stages.

At around 200 Myr the structure of the interstellar matter is relatively ordered, where individual bubbles have merged in a coherent (although far from spherical) expanding super-bubble from which cold ($T < 10^4$ K) filaments protrude inside the cavity. These filaments are the leftovers of previous individual shell-shell interactions further processed by hydrodynamic instabilities. The interactions of expanding hot bubbles give rise to a complex structure in the inner regions, where a metal-rich gas [O/H] = -1.5 coexists with an almost primordial gas. They are separated from each other by cooled shells. After 300 Myr, the halo topology is more perturbed, with bubbles expanding in the outer regions having already

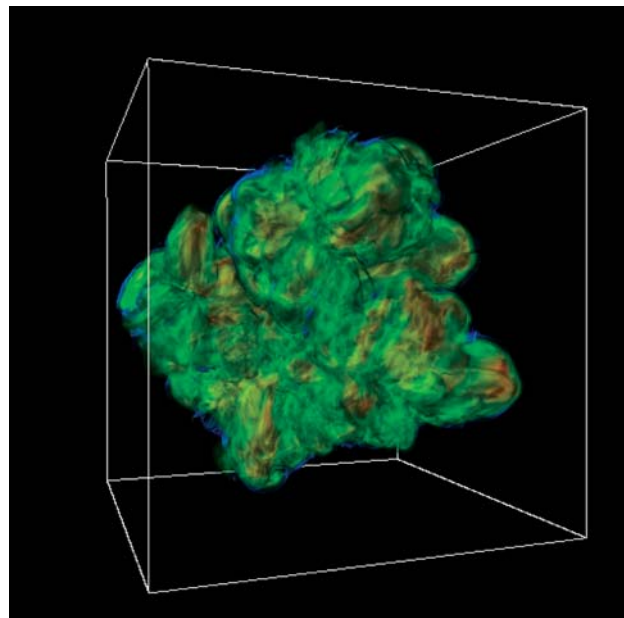


Fig. 7 Three-dimensional distribution of the metallicity [O/H] at the elapsed time of 300 Myr.

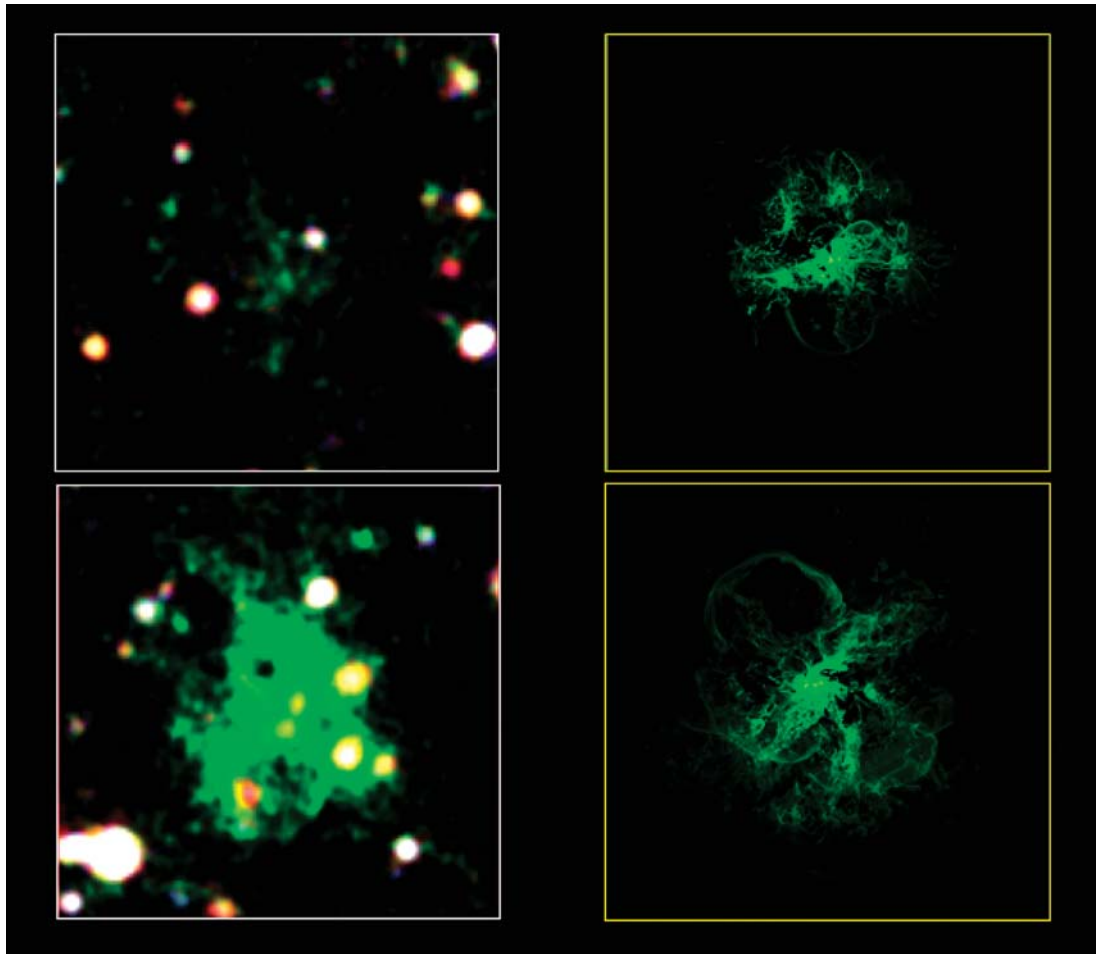


Fig. 8 (Left) $\text{Ly}\alpha$ images of the $\text{Ly}\alpha$ blobs observed by Matsuda et al. (2004) using the Subaru Telescope [4]. (Right) Projected distribution of the $\text{Ly}\alpha$ emission derived by numerical results.

undergone blowout and venting their hot gas into the inter-galactic medium (IGM), and others whose interaction is giving rise to an intricate multiphase structure in the inner halo, where 10^8 K gas coexists with a cooler 10^4 K phase from which it is separated by cooling interfaces. The gas in the vicinity of supernovae is gradually polluted with synthesized heavy elements ejected from supernovae, but a large amount of the gas still retains a low metallicity.

The rightmost panels show the final stages of the evolution. The final stellar system possesses 73% of the initial gas mass. One can clearly see a central, dense core resulting from the interaction of sub-galactic system and the result of the accretion of cold clumps that are raining towards the center. The simulation box is filled with warm ($T < 10^6$ K) and well-mixed gas at a very low density $n < 10^{-4} \text{ cm}^{-3}$ below the mean value for the intergalactic matter. The mixing of heavy elements is nearly completed, and the metallicity of the remaining gas is a sub-solar value ($-1 < [\text{O}/\text{H}] < 0$). The out-flowing gas escapes from the gravitational potential of the whole system and is ejected into the intergalactic space. Figure 7 shows a

three-dimensional distribution of the metallicity $[\text{O}/\text{H}]$ at the elapsed time of 300 Myr. A large fraction of the gas has been swept-up during the evolution. This supernova-driven pregalactic outflow is an efficient mechanism for distributing the product of stellar nucleosynthesis over large cosmological volumes.

Finally, we present the results of “Observation-oriented Visualization” of simulation results. In order to compare the simulation results with observations, we need to observe the numerical results in the same energy band as real observations. We computed the emission properties of the “virtual” galaxy assuming for an optically thin gas in collisional ionization equilibrium and using the MAPPING3 code by Sutherland & Dopita [7]. In practice, to obtain the radiation spectrum of the system we sum up the radiation energy distribution of each grid point.

Let us compare the results of such visualization with recent observations of $\text{Ly}\alpha$ blobs. Matsuda et al. [4] reported the properties of the 35 robust candidates of $\text{Ly}\alpha$ blobs searched in and around the proto-cluster region at redshift $z=3.1$ (3.5 Gyrs from the birth of universe) discovered by Steidel et al. [3] in the SSA22 field with the

prime-focus camera on the Subaru telescope. Two examples of such Ly α blobs are shown in the left panels of figure 8. The size of the Ly α emitting clouds is larger than 100 kpc and much larger than current galaxies. These blobs are snapshots of ongoing galaxy formation. These Ly α blobs do not have ultra-violet sources apparently bright enough to produce the extended photo-ionized Ly α emission line nebulae. The ionization or excitation mechanisms of these Ly α blobs were unclear.

The right panel of figure 8 shows the projected distribution of the Ly α emission computed from the simulation results, where the angular resolution is 1.6×10^{-2} arcsec (corresponding to the numerical resolution, 117pc). We found that the resultant Ly α luminosity can account for the observed luminosity of Ly α blobs; in addition, the bubbly structures produced by multiple supernova explosions are quite similar to the observed features in Ly α surface brightness of Ly α blobs .

3. Summary and Discussion

We presented the results of ultra-high resolution hydrodynamic simulations using 1024^3 grid points which resolve individual supernova remnants in a forming galaxy. The numerical results are synthesized to produce virtual image of the protogalaxy observed by the Ly α emission line. The distribution of the Ly α emission derived by numerical results is similar to the image of the Ly α blobs recently observed by the Subaru Telescope. Our simulations showed that the peak star formation rate is about $40 M_{\odot} \text{ yr}^{-1}$ and the burst of star formation continues to 300 Myr. These results are consistent with the stellar age determinations by recent observations and the inferred star formation rate. Furthermore the simulation successfully reproduced the metallicity of Lyman break galaxies which is mostly subsolar and ranges from [Fe/H] -0.3 to -1 .

We have shown that Ly α Emitters are likely to be young galaxies experiencing major episodes of star formation and the inhomogeneous mixing of heavy elements produces a large spread of metallicities, which affects the subsequent galactic chemical evolution and leaves its imprint on metal-deficient stars. We found that the resultant Ly α luminosity can account for the observed luminosity of Ly α blobs; in addition, the bubbly structures produced by multiple supernova explosions are quite similar to the observed features in Ly α surface brightness of Ly α Emitters. Hence the emerging theoretical picture is fully consistent with observational data. It is concluded

that Ly α Emitters can be identified with primordial galaxies observed in a supernovae-dominated phase.

Acknowledgements

We thank H. Yahagi for supplying us the images of the dark matter distribution obtained by cosmological N-body simulations carried out by using VPP5000 at NAOJ. This work was supported in part by the Grant-in-Aid of the Ministry of Education, Culture, Science, and Sports, 14740132 and 16002003, and by the Promotion and Mutual Aid Corporation for Private Schools of Japan. The numerical computations were carried on the Earth Simulator at the JAMSTEC, using 1024 processors (128 nodes), and the data analysis was done by a parallel computer SPACE at Senshu University using 64 processors.

(This article is reviewed by Dr. Tetsuya Sato.)

References

- [1] H. Yahagi, Parallel N-body Method with Adaptive Mesh Refinement, PhD Thesis, Department of Astronomy, University of Tokyo, 2002.
- [2] C. C. Steidel, K. L. Adelberger, A. E. Shapley, M. Pettini, M. Dickinson, and M. Giavalisco, Ly α Imaging of a Proto-Cluster Region at $z=3.09$, *Astrophys. J.*, vol.**532**, pp.170–182, 2000.
- [3] Y. Ohyama, Y. Taniguchi, K. S. Kawabata, Y. Shioya, T. Maruyama, T. Nagao, T. Takata, M. Iye, and M. Yoshida, On the Origin of Ly α Blobs at High Redshift: Kinematic Evidence of a Hyperwind Galaxy at $z = 3.1$, *Astrophys. J.*, vol.**591**, L9–L12, 2003.
- [4] Y. Matsuda et al., A Subaru Search for Ly α Blobs in and around the Protocluster Region At Redshift $z = 3.1$, *Astronomical Journal*, vol.**128**, pp.569–584, 2004..
- [5] M. Mori, A. Ferrara, and P. Madau, Early Metal Enrichment by Pregalactic Outflows. II. Three-dimensional Simulations of Blow-Away, *Astrophys. J.*, vol.**571**, pp.40–55, 2002.
- [6] K. Wada, and M. S. Liou, AIAA paper, 94-0083, 1994.
- [7] R. S. Sutherland and M. A. Dopita, Cooling functions for low-density astrophysical plasmas, *Astrophys. J. Supplement*, vol.**88**, pp.253–327, 1993.
- [8] T. Tsujimoto, K. Nomoto, Y. Yoshii, M. Hashimoto, S. Yanagida, and F-K. Thielemann, Relative frequencies of Type Ia and Type II supernovae in the chemical evolution of the Galaxy, LMC and SMC, *Mon. Not. Roy. Astron. Soc.*, vol.**277**, pp.945–958, 1995.